PHYSICAL REVIEW D **78,** 115009 (2008)

Study of highly excited string states at the Large Hadron Collider

Douglas M. Gingrich* and Kevin Martell

Centre for Particle Physics, Department of Physics, University of Alberta, Edmonton, AB T6G 2G7 Canada

(Received 25 October 2008; published 15 December 2008)

In TeV-scale gravity scenarios with large extra dimensions, black holes may be produced at future colliders. Good arguments have been made for why general relativistic black holes may be just out of reach of the Large Hadron Collider (LHC). However, in weakly coupled string theory, highly excited string states—string balls—could be produced at the LHC with high rates and decay thermally, not unlike general relativistic black holes. In this paper, we simulate and study string ball production and decay at the LHC. We specifically emphasize the experimentally detectable similarities and differences between string balls and general relativistic black holes at a TeV scale.

DOI: 10.1103/PhysRevD.78.115009 PACS numbers: 04.70.Bw, 04.70.−s, 12.60.−i

I. INTRODUCTION

Models of large extra dimensions [1–3] and experimental constraints [4–9] allow the scale of gravity to be as low as a TeV. At this scale, the intriguing possibility exists that black holes could be produced at the Large Hadron Collider (LHC) and in cosmic-ray events [10–15]. This possibility has been well studied for the case in which the black hole is treated semiclassically, and is produced and decays according to the concepts of general relativity (GR). In this paper, we consider black holes as GR objects, and we will address the issue of what happens below the energy scale at which trans-Planckian objects are no longer considered GR black holes.

Meade and Randall [16] have recently provided a nice summary of the conditions required on the masses of gravitational objects for them to be considered GR black holes. One commonly used condition is that the entropy of the black hole must be greater than 25 in order to fulfill the thermodynamic description of black holes.[1] This leads to the black hole mass production requirement of $M_{\mathrm{BH}} \gtrsim 5M_D$, where M_D is the fundamental Planck scale in higher dimensions. If M_D is about 1 TeV, imposing the GR condition on black holes leads to a requirement on the black hole mass of $M_{\mathrm{BH}} \gtrsim 5$ TeV. Thus, because of this requirement, high mass GR black holes may not be accessible to the LHC. Their production at the LHC will be particularly unlikely if black holes are not produced through totally inelastic collisions and some of the parton energy is not available for black hole formation [17–19].

Because of the steeply falling parton density distributions in the protons with increasing parton center of mass energy, the black hole cross section drops with increasing black hole mass. This means that the most probable black holes produced are those just satisfying the GR condition and thus closest to the fundamental Planck scale. Unfortunately, the most accessible black holes are also the least theoretically understood.

We will define a mass threshold at which black holes can no longer be treated by GR. Below this GR threshold we enter the regime of quantum gravity. In this regime, Meade and Randall [16] have considered black-hole type objects within composite models and have studied the possibility of their decay into dijets (and dileptons). Another exciting possibility for this regime occurs when everything below the GR threshold is treated in the context of weakly coupled string theory. Although string theory is not required in TeV-scale gravity in higher dimensions, it does allow us to postulate how a black hole makes a transition across the GR threshold as it evaporates.

The scenario of large extra dimensions is not a model but rather a paradigm in which models can be built. Although inspired by string theory, the large extra dimensions paradigm is not based on it. However, embedding the large extra dimensions into string theory could provide an understanding of the strong-gravity regime and a picture of the evolution of a black hole at the last stages of evaporation [20]. In this picture, black holes end their Hawking evaporation when their mass reaches a critical mass. At this point they transform into high-entropy string states—string balls—without ever reaching the singular zero-mass limit.

It has been shown that string states produced below the GR threshold could have a cross section comparable to that of the black hole [21–23]. Hence, these states will be even more accessible than black holes at the LHC. Moreover, even if black holes are produced at the LHC, they will evolve into these string states. In themselves, string balls are interesting because they are a new form of matter involving gravity and string theory. However, if large extra dimensions are realized in a string theory of quantum gravity, excited string states of standard model particles will have TeV masses [24–28]. These states could provide the first signatures of low-scale quantum gravity.

Cheung [22], and Chamblin and Nayak [23] calculated large string ball cross sections at the LHC based on the

*Also at TRIUMF, Vancouver, BC V6T 2A3 Canada. gingrich@ualberta.ca

[1]For Schwarzschild black holes, the entropy requirement also ensures that the Compton wavelength of the black hole is less than its horizon radius.

parton cross sections of Dimopoulos and Emparan [21].[2] However, full simulations were not performed, and experimental and background effects were not discussed; that is the goal of this paper. With the startup of the LHC such detailed studies are timely and of value.

This paper is structured as follows. In Sec. II, we summarize the weakly coupled string model of highly excited string states embedded in large extra dimensions. The hierarchy of the energy scales involved are discussed in Sec. III. In Sec. IV, string ball production is described, while in Sec. V, a model for string ball evaporation is developed. Our results are presented in Sec. VI, and a discussion follows in Sec. VII. We do not discuss excited string resonances of standard model particles, nor string effects near or below the string scale in this paper.

II. WEAKLY COUPLED STRINGS

If the energy of parton-parton scattering is comparable to the string scale, the point-particle description of scattering will have to be replaced by a string-string description of scattering. As the energy increases above the string scale, the string states will become highly excited, jagged, and entangled. Such string states are commonly referred to as string balls [21]. Eventually, at high enough energies a transition point is reached in which the string ball turns into a black hole.

Embedding TeV-scale gravity scenarios in realistic string models could enable calculations near M_D. One perturbative string theory with weak-scale string tension is the SO(32) type-I theory having

(1) new dimensions much larger than the weak scale,
(2) $\mathcal{O}(1)$ string coupling,
(3) standard model fields identified with open strings localized on a 3-brane, and
(4) a gravitational sector consisting of closed strings propagating freely in the extra dimensions.

At present, there are no $\mathcal{N}=1$ supersymmetric string models in accordance with the large extra dimensions scenario, that break to only the standard model at low energies without the presence of extra massless particles. However, there are nonsupersymmetric string models that can realize the large extra dimensions scenario and break to only the standard model at low energy with no extra massless matter [30,31].

We will consider a model with n large extra dimensions and $(6-n)$ small extra dimensions. After compactification of the small dimensions to the size of the string length scale, we obtain a relationship between the fundamental Planck scale and the string parameters

$$M_D^{n+2} \sim \frac{M_s^{n+2}}{g_s^2}, \tag{1}$$

where n is the number of large extra dimensions, M_s is the string scale, and g_s is the string coupling. The string coupling constant is determined by the expectation value of the dilaton field. If string theory is perturbative ($g_s < 1$), we see that $M_s < M_D$ for all n. Equation (1) is an equality to order unity. The exact numerical coefficient, which may depend on n, is model dependent. It depends on the string theory and compactification scheme, and would involve one-loop calculations. The value of the numerical coefficient normally does not matter, since M_D and M_s are not well-defined masses but are energy scales at which new phenomena occur. However, for the numerical calculations performed in this paper it is important to take into account all the $\mathcal{O}(1)$ numerical factors in a consistent manner. If the coefficient is greater than unity, then M_D is greater than M_s. If the coefficient is less than unity, there are values of g_s for which M_s is greater than M_D. As in previous work, we shall take the coefficient to be unity, and thus $M_D \geq M_s$. This assumption breaks down only for the case of g_s greater than the coefficient, at which point the "highly excited string" states are actually black hole states.

A. Correspondence principle

According to the string theory of quantum gravity, the minimum mass above which a black hole can be treated general relativistically is [32,33]

$$M_{\min} \sim \frac{M_s}{g_s^2}. \tag{2}$$

The properties of a black hole with mass $M_{\min}$ matches those of a string ball with the same mass. This is called the correspondence principle, and the mass at which this happens is the correspondence point. When a black hole makes a transition to a string it can become a single string, multiple strings, or radiation. The single string configuration dominates, since its entropy is the highest [21,33].

The number of microstates of both black holes and string balls should be the same at the correspondence point. The entropy of a long string is proportional to its mass

$$S_s \sim \sqrt{\alpha'} M = \frac{M}{M_s}, \tag{3}$$

where α' is the slope parameter given in terms of the string tension T as $\alpha' = 1/(2\pi T)$. We have used $\sqrt{\alpha'} = \ell_s = 1/M_s$. At the correspondence point $S_s \sim 1/g_s^2$.

The Bekenstein entropy [34] of a black hole is proportional to its area. The black hole entropy in higher dimensions is

$$S_{\mathrm{BH}} = \frac{4\pi}{n+2} f(n) \left(\frac{M}{M_D}\right)^{(n+2)/(n+1)} \sim \frac{4\pi}{n+2} f(n) \frac{1}{g_s^2} \left(\frac{g_s^2 M}{M_s}\right)^{(n+2)/(n+1)}, \tag{4}$$

where

[2] String ball production has also been discussed in the context of ultrahigh energy neutrinos in cosmic radiation [29].

$$f(n) \equiv \left[\frac{2^n \pi^{(n-3)/2}\Gamma(\frac{n+3}{2})}{n+2}\right]^{1/(n+1)} \quad (5)$$

is an n-dependent factor of $\mathcal{O}(1)$. In the last expression of Eq. (4), we have used the relationship between the fundamental Planck scale and the string parameters given by Eq. (1). At the correspondence point $S_{\rm BH} \sim 1/g_{\rm s}^2$ and is equal to the string entropy at the correspondence point to within a numerical coefficient. The black hole and string entropies have the same mass dependence near the correspondence point but the numerical coefficient is unknown. A better understanding of the string state near the string scale would be required to precisely determine the coefficient.

The coefficient multiplying the correspondence point in Eq. (2) is usually considered to be a factor of order unity. The factor represents exactly when the string state forms a black hole. The factor depends on the string theory in terms of its entropy and the relationship between the string scale and the fundamental higher-dimensional Planck scale. For a factor of unity, the black hole entropy is always smaller than the string entropy at the correspondence point for common superstring theories. We will take the coefficient in Eq. (2) to be unity as in previous studies. If this assumption is invalid and the coefficient is much less than unity, the energy range in which the effects of quantum gravity are important will be very narrow. If the coefficient is much larger than unity, black holes are unlikely to be observed at the LHC even if the Planck and string scales are around a TeV.

Although the correspondence principle has worked well in four dimensions when numerical coefficients have been dropped, it has not worked so well for a consistent set of coefficients in higher dimensions. Halyo et al. [35] could not get an exact match between the four-dimensional Schwarzschild or nonextreme charged black holes and any fundamental string theory. Solodukhin [36] obtained matching by adding a logarithmic quantum correction to the black hole entropy. A gravitation term was then added to the string entropy to get exact matching of the two terms in the black hole entropy. Adding the extra degrees of freedom allowed matching. This matching only works in four dimensions where the self-interactions are an integer power series in $g_{\rm s}$.

Presumably, we must match the black hole entropy to the interacting string entropy rather than the free entropy. It is natural to identify the ''internal states'' of the black hole not with states of the free string but with a part of the states of the interacting string. We can consider the string entropy as a perturbation series with respect to $g_{\rm s}$. In principle, the string entropy could possess some nonperturbative corrections, behaving as $\sim 1/g_{\rm s}^2$.

It is also possible that the black hole states can only turn into a subset of the available string states. If the subset is large enough, the entropies should only differ by a numerical coefficient of order unity. Thus, a one-to-one correspondence between black hole states and string states my not be necessary.

B. Random-walk string

The black hole's size at the correspondence point is of the order of the string length scale $\ell_{\rm s}$. By contrast, long excited string states are a chain of connected string bits, each with length equal to $\ell_{\rm s}$. An excited string has a tendency to spread out as in a random walk. Since one end of each string bit will perform a random walk relative to the other, the size of these objects must be calculated statistically. The step size of the random walk is $\ell_{\rm s}$, and its total length is $(M/M_{\rm s})\ell_{\rm s}$, so the mean radius of the average configuration of mass M (i.e. the radius of the string ball) is [37,38]

$$R_{\rm rw} \sim \sqrt{\frac{M}{M_{\rm s}}}\ell_{\rm s} \sim \sqrt{M}\ell_{\rm s}^{3/2} > \ell_{\rm s}. \quad (6)$$

However, this neglects the gravitational self-interaction of the string. This is responsible for keeping the string compact at a size of about $\ell_{\rm s}$ near the correspondence point. Hence, shortly after the black hole to string ball transition, the string abruptly ''puffs up'' from string length scale size $\ell_{\rm s}$ to random-walk size $R_{\rm rw}$.

At the LHC, the puff up might not be too large or happen at all. That is, the black hole horizon radius at the correspondence point is $f(n)\ell_{\rm s}$, where $f(n) = 1.3$–2.4 for $n = 3$–6, while the maximum random-walk string size is about $\ell_{\rm s}/g_{\rm s}$. Thus, for small values of $g_{\rm s}$, the puff up would not occur.

III. ENERGY SCALES

The production of black holes and string states depends on four free parameters $M_{\rm s}$, $g_{\rm s}$, n, and M_D. Typically,

$$M_{\rm s} < M_D < \frac{M_{\rm s}}{g_{\rm s}} < \frac{M_{\rm s}}{g_{\rm s}^2}. \quad (7)$$

Later on, we will see that $M_{\rm s}/g_{\rm s}$ divides the regions between perturbative string theory and unitarity. Figure 1 displays a possible hierarchy of energy scales at the LHC.

For GR black holes, we require their mass $M_{\rm BH} \geq \zeta M_D$, and thus using Eq. (2)

$$M_{\rm min} = \frac{M_{\rm s}}{g_{\rm s}^2} = \zeta M_D. \quad (8)$$

FIG. 1. Energy scales for black holes and string balls in the context of the LHC energy. Not shown are the compactification scale or the ultraviolet cutoff scale.

Normally, we will take $\zeta \sim 5$ as required by the thermodynamic and Compton wavelength arguments given in Sec. I. However, $\zeta \sim 3.4$ is acceptable for higher dimensions. If the unit coefficient in Eq. (2) is invalid, it can somewhat be compensated for by the choice of ζ. If the assumed ζ is too low, black hole production will be overestimated, and string ball production will be slightly underestimated in this paper.

It is not known how much higher above M_s the energy must be in order to be in the stringy regime, where random-walk string states are valid. As M/M_s drops to unity this picture will no longer be valid. We take

$$M_{SB} > 3M_s \tag{9}$$

as a requirement for the validity of the long and jagged picture of string balls. The exact location of this low-energy cutoff mainly affects integrated cross sections. Most of the results in this paper are insensitive to this choice of cutoff provided it is not too large, in which case neither string balls nor black holes will be observable at the LHC.

If string theory is strongly coupled ($g_s \sim 1$), all the scales would be about the same. In this case, black-hole-like behavior will appear at the scale M_D, and all the string states will be black hole states. For very weak string coupling ($g_s \ll 1$), string ball production occurs at very high energies, and there would be no black hole production at the LHC. For moderate values of g_s there is a significant energy range between M_s and M_{min} inside which the spectrum is intrinsically stringy and the GR approximation fails. The fundamental Planck scale M_D is typically smaller than M_{min}, so the GR approximation can fail even above M_D. We will consider g_s moderately less than unity and thus a significant stringy regime between the scales M_s and M_{min} can occur.

Virtual graviton effects depend on the ultraviolet cutoff of the Kaluza-Klein spectrum. Since the fundamental Planck scale in models of large extra dimensions is $M_D \sim 1$ TeV, it is natural to expect this cutoff to be of the same order. It is possible that the ultraviolet cutoff is somewhat lower than M_D. We will take an operational approach of considering M_s to be the lowest energy scale at which the first effects of gravity would be observed in experiments. This approach requires M_s to be consistent with experimental limits on gravitational effects and thus $M_s \gtrsim 1$ TeV.

Using the two constraints [Eq. (1) and (8)] between M_s, g_s, n, and M_D, the string ball characteristics depend on two independent parameters; we normally choose M_s and n. Although M_D is the more common independent scale, by using M_s we are working with the lowest energy scale. All higher energy scales will be determined by the constraints as well as the string coupling. The string coupling and Planck scale are determined by

$$g_s^2 = 1/\zeta^{(n+2)/(n+1)}, \tag{10}$$

and

$$M_D = \zeta^{1/(n+1)} M_s. \tag{11}$$

The choice of $\zeta = 5$ keeps the values for g_s in the perturbative regime and M_D consistent with experimental limits. Table I shows values for the parameters g_s, M_D, M_s/g_s, and M_s/g_s^2 when $M_s = 1$ TeV and $\zeta = 5$. The significance of M_s/g_s will be explained in the next section. Also shown in Table I are values of $f(n)$ given by Eq. (5), which are often ignored.

IV. STRING BALL PRODUCTION

The correspondence principle also suggests that the production cross section for string balls will match the black hole cross section at center of mass energies around M_s/g_s^2

$$\sigma(\mathrm{SB})|_{M_{SB}=M_s/g_s^2} \sim \sigma(\mathrm{BH})|_{M_{BH}=M_s/g_s^2}. \tag{12}$$

Because the black hole size near the correspondence point is smaller than the excited string size, the transition may involve the effects of strong self-gravity around this energy [38].

The production cross section for string balls with mass between the string scale M_s and M_s/g_s grows with the center of mass energy squared $\hat{s} = M^2$ as [21]

$$\sigma_s \sim \frac{g_s^2}{M_s^4} M^2. \tag{13}$$

This expression generalizes to arbitrary dimensions as a consequence of the independence of the string scattering amplitude on dimensions.

Most scenarios of low-scale quantum gravity as low-energy effective theories are valid only up to order M_s. Above this scale, the naive calculations typically violate perturbative unitarity. The unitarity bound for Eq. (13) occurs at $g_s^2 \hat{s}/M_s^2$ [39]. Thus, the production cross section for string balls grows with M^2 only for $M_s < M \leq M_s/g_s$. One has to introduce some *ad hoc* unitarization scheme, since a fundamental string theory is still unavailable. At the unitarity point M_s/g_s, the string cross section is

$$\sigma_s = \frac{1}{M_s^2}. \tag{14}$$

We thus take the string ball cross section to be constant between M_s/g_s and M_s/g_s^2. The proton-proton cross sec-

TABLE I. Parameter values for $M_s = 1$ TeV and $\zeta = 5$.

n	g_s	M_D [TeV]	M_s/g_s [TeV]	M_s/g_s^2 [TeV]	f
2	0.34	1.7	2.9	8.6	0.90856
3	0.37	1.5	2.7	7.5	1.33746
4	0.38	1.4	2.6	6.9	1.73470
5	0.39	1.3	2.6	6.5	2.10164
6	0.40	1.3	2.5	6.3	2.44219

tion for string ball production is dominated by the parton density functions at low production masses. Thus, if the assumptions in Eq. (14) are incorrect and the cross section continues to rise slowly, this effect will be hard to detect in experimental data. The exact coefficient (normalization) is a question to be determined by experiment.

The approximate match between this constant cross section and that of a black hole at the correspondence point becomes obvious when using the relationship between M_D and M_s given by Eq. (1) in the black hole cross section

$$\sigma_{\rm BH} = \pi \frac{f^2(n)}{M_D^2}\left(\frac{M}{M_D}\right)^{2/(n+1)} \to \pi \frac{f^2(n)}{M_s^2}\left(\frac{g_s^2 M}{M_s}\right)^{2/(n+1)} \sim l_s^2\left(\frac{g_s^2 M}{M_s}\right)^{2/(n+1)}, \quad (15)$$

where we have dropped numerical coefficients in the last expression.

Including the n-dependent coefficient for the black hole cross section, the parton cross section over all three energy regions is

$$\hat{\sigma} = \begin{cases} \frac{g_s^2 M^2}{M_s^4} & M_s \ll M \le \frac{M_s}{g_s}, \\ \frac{1}{M_s^2} & \frac{M_s}{g_s} \le M \le \frac{M_s}{g_s^2}, \\ \pi \frac{f^2(n)}{M_D^2}\left(\frac{M}{M_D}\right)^{2/(n+1)} & \frac{M_s}{g_s^2} < M. \end{cases} \quad (16)$$

The lower two energy ranges lead to string ball production and the higher one leads to black hole production.

Dimopoulos and Emparan [21] considered the cross sections to within only numerical factors. This allowed them to match the cross sections at the correspondence point but changed the standard black hole cross section. Cheung [22] multiplied the string cross sections by the n-dependent numerical factor $f^2(n)$ to obtain matching. This resulted in string cross sections that depended on the number of large extra dimensions in an arbitrary way.

The cross section should contain Chan-Paton factors [40], which control the projection of the initial state onto the string spectrum [25]. In general, this projection is not uniquely determined by the low-lying particle spectrum. This is usually accounted for by introducing one or more arbitrary constants. Besides g_s and M_s, the Veneziano amplitudes are characterized by two constants, which parameterize the Chan-Paton traces for string models. Thus, the overall coefficient in the cross section, Eq. (13), is unknown, and we will take it to be unity. The exact value of the cross section is an experimental issue.

The saturation cross section is $1/M_s^2$. If exact continuity of the cross section is required, the correspondence point will occur at very low energy. For all n values, the correspondence point will be so low that it rules out string ball production at the LHC. A discontinuity in the cross section is not physical but with a better knowledge of the strong gravitational effects, we could expect the transition to be smooth.

V. STRING BALL EVAPORATION

Highly excited long strings (averaged over degenerate states of the same mass) emit massless (as well as massive) particles with a thermal spectrum at the Hagedorn temperature [41]. Hence, the conventional description of evaporation in terms of blackbody emission can be applied to highly excited string states. Assuming a type-I string theory, the emissions can take place either in the bulk (into closed strings) or on the brane (into open strings).

The Hagedorn temperature is given by

$$T_s = \frac{M_s}{\sqrt{8}\pi}. \quad (17)$$

The temperature is the same for evaporation to open strings on the brane or closed strings in the bulk. The Hagedorn temperature can be viewed as either the maximum temperature or the temperature of a phase transition. However, one should be aware that the concept of temperature and phase transition are ill-defined in the presence of gravity.

To leading order, the formal temperature, given by $T = (\partial S/\partial M)^{-1}$, is usually equal to the Hagedorn temperature. The formal temperature for a free string includes a mass dependent term coming from a logarithmic term in the entropy. This term raises the temperature for small masses. The entropy could also include self-gravity and fixed-size terms. Since strings emit particles with a thermal spectrum at the Hagedorn temperature and not the formal temperature, we will ignore any extra terms in the temperature.

The Hawking temperature for black hole evaporation in higher dimensions is

$$T_{\rm H} = \frac{n+1}{4\pi}\frac{1}{R_h} = \frac{n+1}{4\pi f(n)}\left(\frac{M_D}{M}\right)^{n+1} M_D \to \frac{n+1}{4\pi f(n)}\left(\frac{1}{g_s^2}\right)^n M_s, \quad (18)$$

where the last expression is the maximum temperature at the correspondence point. Similarly to the entropy and cross section, the Hagedorn temperature of an excited string matches the Hawking temperature of a black hole at the correspondence point. In the random-walk phase, the string still evaporates at the Hagedorn temperature, which eventually brings the size down toward ℓ_s. Even if black holes are produced at the LHC, the black holes will decay into string balls, and eventually down to low-lying string states.

The Hagedorn temperature in Eq. (17) is for a free string. Perturbative corrections to that temperature could be expected. For a highly excited, weakly coupled, neutral string, the leading order term in perturbation theory is just the Hagedorn temperature at which a very weakly coupled string will radiate. Thus, the temperature of a string at a large level number would have a perturbation expansion of the form

$$T = T_s + g_s^2 F(M) + \cdots. \tag{19}$$

The black hole decays mainly on the brane [42]. The emissivity depends not only on the temperature (and thus mass) but also weakly on the total number of space-time dimensions. An equal amount of radiation will be emitted into the Kaluza-Klein tower of a single bulk species as will be emitted into a single brane species. Including the number of degrees of freedom at the LHC, the bulk emission is notable but still not dominant [43,44].

The decay depends not only on the temperature but also on the D-dimensional area of the object emitting Hawking radiation. For black holes and random-walk strings, the area is well defined. Moreover, because there is no relationship between the physical size of the string and its temperature, to first order, the decay may be different from that of a black hole. To examine this, we follow the arguments of Emparan, Horowitz, and Myers [42] but apply them to random-walk strings. In D dimensions, the energy radiated by a blackbody of temperature T and surface area A_D is

$$\frac{dE_D}{dt} = \sigma_D A_D T^D, \tag{20}$$

where σ_D is the D-dimensional Stefan-Boltzmann constant given by

$$\sigma_D = \frac{\Omega_{D-3}}{(2\pi)^{D-1}(D-2)}\Gamma(D)\zeta(D), \tag{21}$$

where $\zeta(D)$ is the Riemann zeta function, Ω_D denotes the volume of a unit D-sphere, and $A_D = r^{D-2}\Omega_{D-2}$ is the area of the string of radius r.

The ratio of emissivities in D dimensions to four dimensions is given by

$$\frac{\dot{E}_D}{\dot{E}_4} \sim \left(\frac{1}{\sqrt{8}\pi}\right)^n \left(\frac{M}{M_s}\right)^{n/2}, \tag{22}$$

where the omitted numerical coefficient increases from 1 to about 3 as n increases from 0 to 6. Shown in Fig. 2 is the ratio of emissivities. We see that the emissivity ratio is always less than unity at the LHC. Only when $M \gtrsim 56M_s$ will the string radiate more into a single bulk mode; this corresponds to $g_s < 0.13$.

Just below the correspondence point, the string size is a maximum and the ratio of emissivities becomes

$$\left[\frac{\dot{E}_D}{\dot{E}_4}\right]_{\max} \sim \left(\frac{1}{\sqrt{8}\pi g_s}\right)^n. \tag{23}$$

Thus, $g_s \lesssim 1/(\sqrt{8}\pi) = 0.1$ for the bulk modes to dominate. This result was mentioned in Ref. [21]. The result is different from Fairbairn's [45] who ignored all n-dependent coefficients.

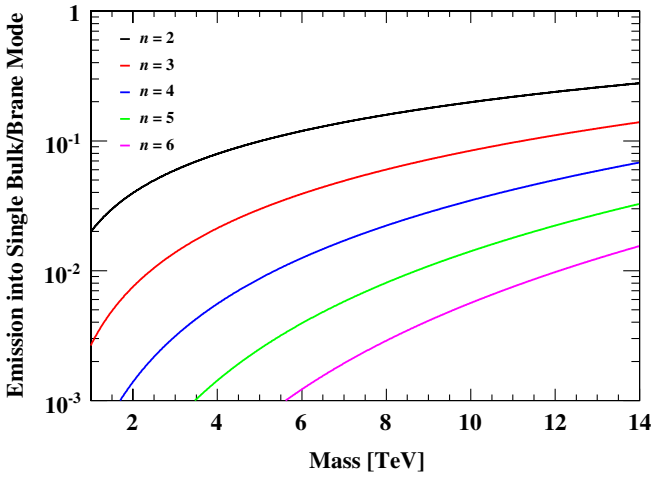

FIG. 2 (color online). Ratio of emission into a single bulk mode to a single brane mode for highly excited strings. The ratio decreases with increasing n.

VI. RESULTS

In this section, we present the results of a study of string balls at the LHC based on the previously described model. The black hole and string ball parton cross sections were given in Eq. (16). However, only a fraction of the total center of mass energy $\sqrt{s}$ in a proton-proton collision is available in the parton scattering process. The total cross section can be obtained by convoluting the parton-level cross section with the parton distribution functions, integrating over the phase space, and summing over the parton types. In this paper, we assume all the available parton energy $\sqrt{\hat{s}}$ goes into forming the black hole or string ball. Although this might be unlikely, it avoids confusing the effects from totally inelastic string ball production with unknown inelastic effects. Also, throughout this paper proton-proton collisions at 14 TeV center of mass energy are considered. When referring to string ball production it is usually understood to also include black hole production if the initial parton energy is high enough.

Throughout this paper we use the CTEQ6L1 (leading order with leading order α_s) parton distribution functions [46] within the LHAPDF framework [47]. The momentum scale for the parton distribution functions is set equal to the black hole or string ball mass for convenience. The extrapolation of the parton distribution functions into the trans-Planckian or "trans-stringian" region based on standard model evolution from present energies is questionable, since the evolution equations neglect gravity.

Figure 3 shows the total proton-proton cross section versus Planck scale for the production of black holes and string balls for various numbers of extra dimensions n. We see that the string ball plus black hole cross sections are at least an order of magnitude higher, and that a substantially enhanced range of M_D could be probed with string balls at the LHC. The black hole cross section is weakly dependent

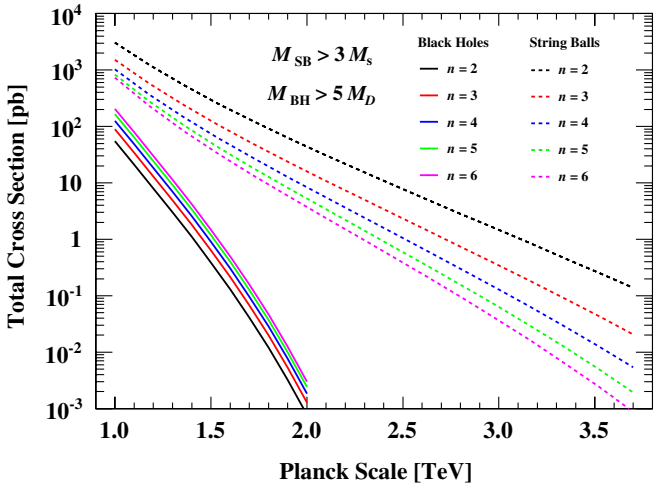

FIG. 3 (color online). Total proton-proton cross section versus Planck scale for the production of black holes (solid curves) and string balls plus black holes (dashed curves) for various numbers of extra dimensions n. The black hole cross section increases with increasing n. The string ball cross section decreases with increasing n.

on n, while the n dependence of the string ball cross section is mainly due to the n-dependent relationship between the string scale and the Planck scale Eq. (11).

Figure 4 shows the total proton-proton cross section versus string scale for the production of black holes and string balls for various numbers of extra dimensions n. We see that the string ball plus black hole cross sections are about 1 to 3 orders of magnitude higher, and that a substantial range of M_s could be probed with string balls. The black hole cross sections are strongly dependent on n because of the additional dependence on the relationship

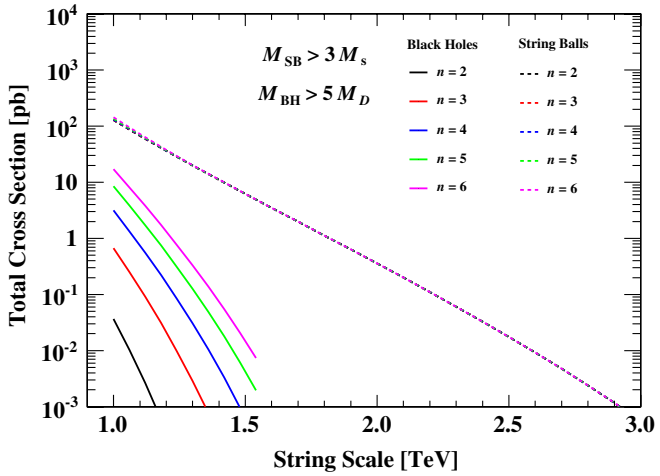

FIG. 4 (color online). Total proton-proton cross section versus string scale for the production of black holes (solid curves) and string balls plus black holes (dashed curves) for various numbers of extra dimensions n. The black hole cross section increases with increasing n.

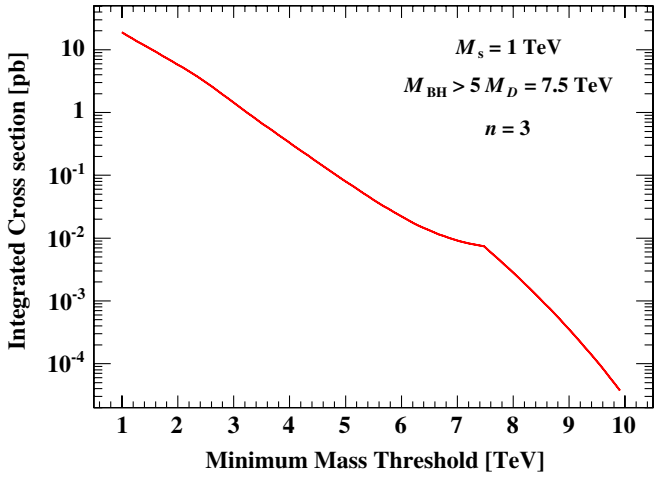

FIG. 5 (color online). Integrated proton-proton cross section versus minimum mass threshold for the production of black holes and string balls plus black holes for three extra dimensions.

between the string scale and the Planck scale Eq. (11). The very weak dependence of the string ball cross section on n is mostly due to the g_s dependence of the string ball cross section below the unitarity point, which depends on n via Eq. (10).

When searching for high-mass states above or near the Planck scale experimentally, one is likely to search for an excess of events above a certain invariant mass threshold. Thus, an important quantity is the integrated cross section above some mass threshold. Figure 5 shows the integrated cross section versus minimum mass threshold for $n = 3$ extra dimensions. Clearly visible is the correspondence point at 7.5 TeV, and not so visible is the unitarity limit at 2.7 TeV. Cross section values for masses less than about $3M_s$ may not be reliable.

Figure 5 shows that for $n = 3$ and $M_D = 1.5$ TeV, the integrated cross section for black hole production is about 10 fb. Assuming a detector efficiency of 0.1, about 10 fb^{-1} of data might be required to discover or rule out GR black holes with these parameters.[3] Since the integrated cross section for string ball production at $3M_s = 3$ TeV is about 1 pb, the equivalent search for string balls might require about 100 times less data.

To simulate string ball production and decay, we started from a modified version of the Monte Carlo event generator CHARYBDIS version 1.003 [49] and adapted it for our

[3]An acceptance of 0.1 is reasonable since early Monte Carlo estimates using the ATLAS detector indicate that an acceptance of about 0.17 can be obtained by optimizing a set of cuts to enhance the signal to background [48]. To claim a discovery, we might require an excess of 10 events above background and thus the required luminosity would be 10 fb^{-1}. Correspondingly, if no events are observed above background and systematic uncertainties are allowed for, about 10 fb^{-1} of data would be required to rule out a 10 fb cross section at the 95% confidence level.

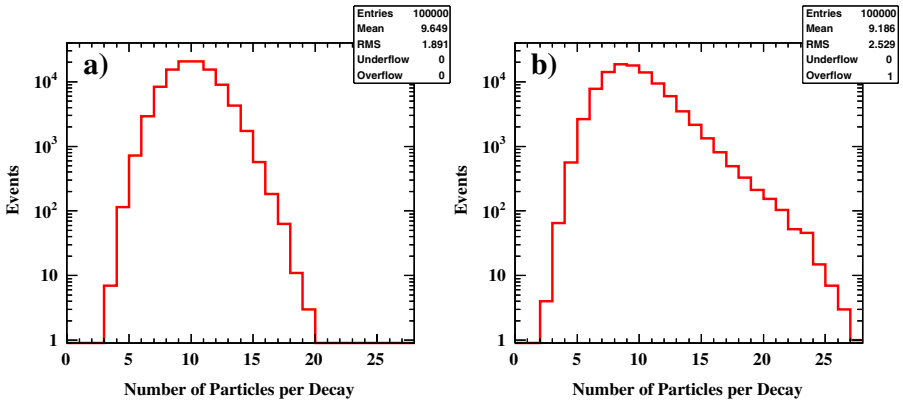

FIG. 6 (color online). Multiplicity distribution of visible primary particles emitted from a) black holes with $7.5 < M < 14$ TeV and b) string balls and black holes with $3 < M < 14$ TeV, for $n = 3$, $M_s = 1$ TeV, $M_D = 1.5$ TeV, and $g_s = 0.37$.

study. The previous modifications were those described in Ref. [44], which included the addition of gravitons, black hole recoil transverse to the 3-brane, and brane tension resisting the black hole from leaving the brane. For the purposes of this study, the string cross section was added to CHARYBDIS, along with the string parameters and the constraints between them. These additions were verified by reproducing all the cross section plots in this paper. For the decays, the Hagedorn temperature for string ball decay replaced the Hawking temperature for black hole decay. The gray-body factors have been used in the results presented here. The number of particle degrees of freedom and the probability for the emission of each degree of freedom was not changed from Ref. [49].

In the previously modified version of CHARYBDIS, the brane tension was a free parameter. By using string theory, we now have a model in which to predict this tension. The 3-brane tension (D-brane tension) is given by [50,51]

$$T = \frac{M_s^4}{(2\pi)^3 g_s}. \tag{24}$$

For $M_s = 1$ TeV, $M_D = 1.5$ TeV, and $g_s = 0.37$, the dimensionless brane tension in units of M_D is 2.2×10^{-3}. For these parameters, there is about a 2% probability for the black hole or string ball to leave the brane according to the model in Ref. [44]. To avoid confusion between string ball effects and recoil effects, we do not simulate graviton emission or black hole recoil in the remainder of our studies.

In the following set of figures we will compare the experimentally observable characteristics of black holes and string balls. Figure 6 shows the multiplicity distributions for black holes and string balls for $n = 3$ extra dimensions. Counted in the multiplicity are only primary visible particles (no neutrinos) evaporated from the black hole or string ball. Decays of the primary particles are not counted. The mean multiplicities are similar but the most probable number of particles evaporated from the string ball is about one particle less. This is probably due to the higher temperature of the string ball. The string ball is capable of producing a maximum multiplicity of about seven particles higher than black holes. This is an infrequent occurrence but probably represents initial black hole

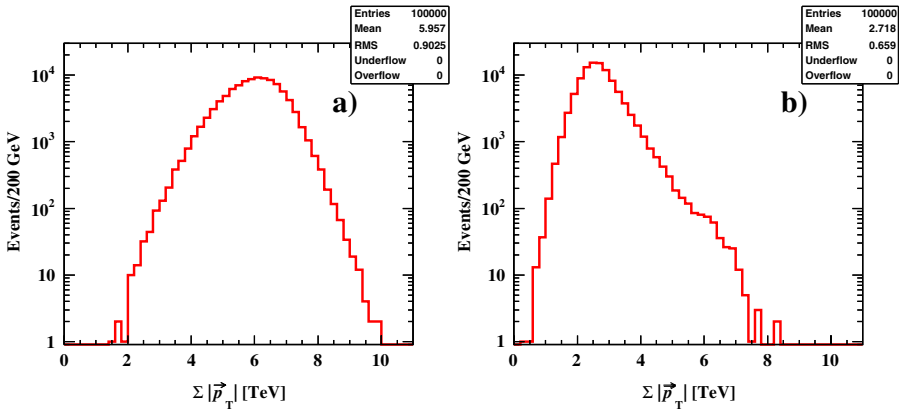

FIG. 7 (color online). Scalar sum of transverse momentum of all the visible particles from a) black holes with $7.5 < M < 14$ TeV and b) string balls and black holes with $3 < M < 14$ TeV, for $n = 3$, $M_s = 1$ TeV, $M_D = 1.5$ TeV, and $g_s = 0.37$.

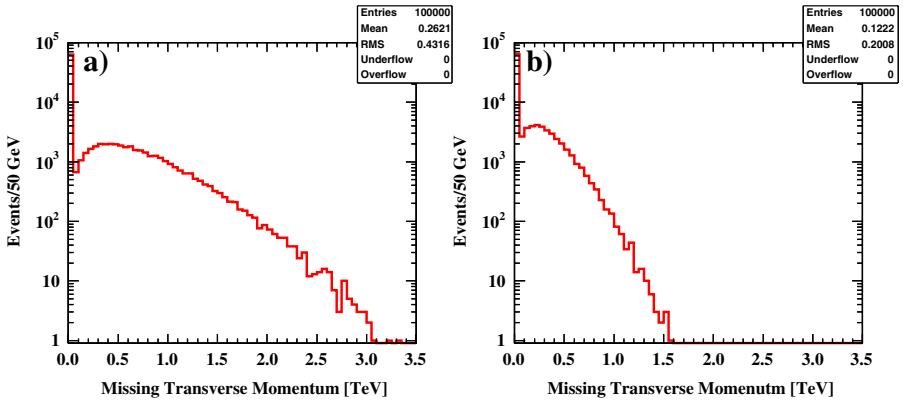

FIG. 8 (color online). Missing transverse momentum in a) black holes events with $7.5 < M < 14$ TeV and b) string balls and black holes events with $3 < M < 14$ TeV, for $n = 3$, $M_s = 1$ TeV, $M_D = 1.5$ TeV, and $g_s = 0.37$.

production followed by decay to a string ball. An experimental requirement of a large number of objects in an event for black hole searches should also be a good requirement for string ball searches.

Figure 7 shows the distribution of the scalar sum of the transverse momentum of each primary particle i, $\sum_i |\vec{p}_T|_i$, for black hole and string ball events. The mean drops from about 6 TeV for black hole events to about 2.7 TeV for sting ball events.

Figure 8 shows the missing transverse momentum distribution in black hole and string ball events. In this parton-level study, missing energy is due to electron, muon, and tau neutrinos, and their antineutrinos. The missing transverse momentum in string ball events is about one half of that in black hole events, and is comparable to that resulting in some supersymmetric models.

Figure 9 shows the transverse momentum p_T of the highest transverse momentum jet in each event for black hole and string ball decays. In this parton-level study, a jet is defined to be a quark, antiquark, or gluon. The average highest-p_T jet in string ball events is about 600–700 GeV lower than in black hole events. The maximum jet p_T in string ball events is about one half of that in black hole events.

Figure 10 shows the transverse momentum p_T of the highest transverse momentum lepton in each event for black hole and string ball decays. In this parton-level study, a lepton is defined to be an electron, muon, or their antiparticles. The average highest-p_T lepton in string ball decays is about 100–200 GeV lower than in black hole decays. The maximum lepton p_T in string ball decays is about one half of that found in black hole decays.

To discuss the standard model backgrounds to string ball production, we rely on Ref. [48]. Studying the backgrounds using a particle-level simulation would have limited validity. Potential standard model backgrounds to string ball events are processes with large cross sections and multiple jets in the event, such as top-quark production, QCD multijet production, as well as Z and W production in combination with multiple jets.

Since string balls (or black holes) are produced in the s-channel and have high invariant mass, $\sum_i |\vec{p}_T|_i$ is also large. Requiring $\sum_i |\vec{p}_T|_i > 2$–3 TeV significantly reduces all but the QCD background and leaves a negligible top-quark

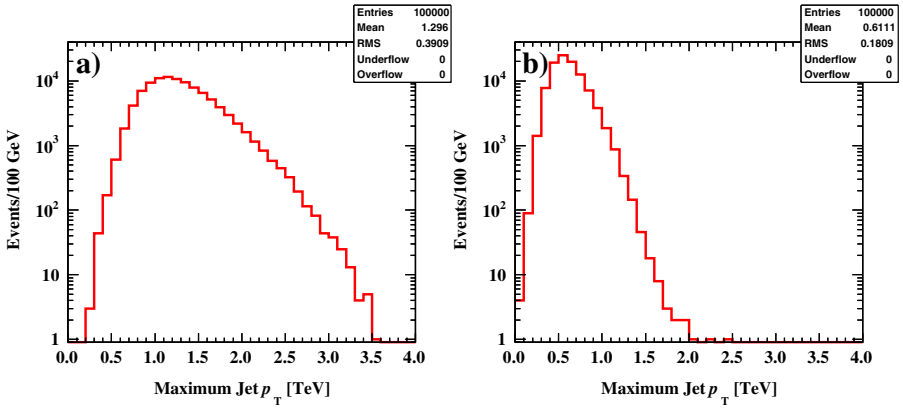

FIG. 9 (color online). Distribution of the highest transverse momentum jet from the decays of a) black holes with $7.5 < M < 14$ TeV and b) string balls and black holes with $3 < M < 14$ TeV, for $n = 3$, $M_s = 1$ TeV, $M_D = 1.5$ TeV, and $g_s = 0.37$.

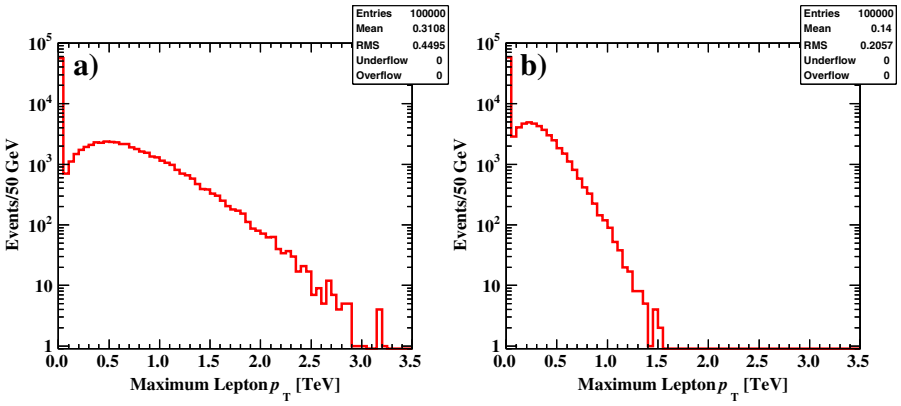

FIG. 10 (color online). Distribution of the highest transverse momentum lepton from the decays of a) black holes with $7.5 < M < 14$ TeV and b) string balls and black holes with $3 < M < 14$ TeV, for $n = 3$, $M_s = 1$ TeV, $M_D = 1.5$ TeV, and $g_s = 0.37$.

background. The QCD background is significantly reduced but, because of its high cross section, a small residual background remains. Figure 7 shows that in searches for string ball events it will be much more difficult to reduce backgrounds due to top-quark events and QCD events by restricting $\sum_i |\vec{p}_T|$, while maintaining a reasonable acceptance for string ball events.

To reduce the background further one can require multiple high-p_T jets in the event. Figure 9 shows that it will be more difficult to reduce backgrounds using high-p_T jet requirements in string ball searches. While a requirement of $p_T > 200$ GeV would be useful in black hole events [48], such a requirement applied to string ball events would be detrimental to the search.

As a final requirement to further reduce the QCD background, a high-p_T lepton requirement can be imposed. The probability of producing a high-p_T lepton in QCD events is small. Requiring a lepton (electron or muon) with $p_T >$ 50–100 GeV reduced the QCD background to a negligible level and reduced the black hole single by less than one half. Figure 10 shows that it will be more difficult to maintain a high efficiency, while reducing backgrounds using a high-p_T lepton requirement in string ball searches.

VII. DISCUSSION

To search for general relativistic black holes at the LHC one will have to look above a certain minimum invariant mass threshold. This threshold can become high relative to typical parton-parton center of mass energies at the LHC if the fundamental Planck scale is a few times higher than its current lower bound. If one tries lowering the threshold, the general relativistic description of black holes breaks down and a quantum gravity description is needed.

One candidate for quantum gravity is weakly coupled string theory. By embedding string theory in large extra dimensions it is possible to predict the occurrence of highly excited string states above the fundamental string scale. According to the correspondence principle these string states match those of a black hole at the energy in which a black hole can no longer be considered as a general relativistic object. Thus, string theory allows us to lower the minimum invariant mass threshold and search for string balls with properties not unlike those of general relativistic black holes. Furthermore, these string balls are the very objects in which the general relativistic black holes will turn into as they evaporate and make a transition across the mass threshold.

Lowering the minimum invariant mass threshold will enhance the search range for trans-Planckian objects near the fundamental Planck scale. However, the consequences of this will be a severely enhanced background from standard model physics processes and supersymmetry, if discovered at a TeV scale. Typical search signatures for general relativistic black holes will involve 1) multiple high-p_T objects (jets, leptons, and photons), 2) high energy in the events, measurable by $\sum_i |\vec{p}_T|_i$, 3) large missing energy, 4) spherical event shapes, etc. [48]. While all of these quantities are significantly higher in general relativistic black hole events than in typical standard model events, this will not be true for string balls, unless the string scale is significantly higher than about 1 TeV, but not too high as to exclude them from being produced at the LHC.

Some might consider the paradigm of large extra dimensions to be unlikely, and the possibility of producing black holes, let alone string states, to be highly unlikely. However, those same people should admit that current experimental bounds on fundamental parameters and searches have not yet ruled out their possibility at the LHC. On the other hand, black holes offer some of the most interesting and broadest manifestations of fundamental physical principles. There is no reason to believe that highly excited string states would not also offer just as rich physics. It is for these reasons that searches for general relativistic black holes and other trans-Planckian phenomena must be initially taken seriously. This paper provides a framework to allow experimentalists to develop

search strategies for highly excited string states within the context of weakly coupled string theory embedded in large extra dimensions.

ACKNOWLEDGMENTS

This work was supported in part by the Natural Sciences and Engineering Research Council of Canada.

[1] N. Arkani-Hamed, S. Dimopoulos, and G. Dvali, Phys. Lett. B **429**, 263 (1998).
[2] I. Antoniadis, N. Arkani-Hamed, S. Dimopoulos, and G. Dvali, Phys. Lett. B **436**, 257 (1998).
[3] N. Arkani-Hamed, S. Dimopoulos, and G. Dvali, Phys. Rev. D **59**, 086004 (1999).
[4] D. J. Kapner, T. S. Cook, E. G. Adelberger, J. H. Gundlach, B. R. Heckel, C. D. Hoyle, and H. E. Swanson, Phys. Rev. Lett. **98**, 021101 (2007).
[5] A. Heister *et al.* (ALEPH Collaboration), Eur. Phys. J. C **28**, 1 (2003).
[6] J. Abdallah *et al.* (DELPHI Collaboration), Eur. Phys. J. C **38**, 395 (2005).
[7] P. Achard *et al.* (L3 Collaboration), Phys. Lett. B **587**, 16 (2004).
[8] A. Abulenica *et al.* (CDF Collaboration), Phys. Rev. Lett. **97**, 171802 (2006).
[9] V. M. Abazov *et al.* (DØ Collaboration), Phys. Rev. Lett. **101**, 011601 (2008).
[10] P. C. Argyres, S. Dimopoulos, and J. March-Russell, Phys. Lett. B **441**, 96 (1998).
[11] T. Banks and W. Fischler, arXiv:hep-th/9906038v1.
[12] S. Dimopoulos and G. Landsberg, Phys. Rev. Lett. **87**, 161602 (2001).
[13] S. B. Giddings and S. Thomas, Phys. Rev. D **65**, 056010 (2002).
[14] J. L. Feng and A. D. Shapere, Phys. Rev. Lett. **88**, 021303 (2001).
[15] L. A. Anchordoqui, J. L. Feng, H. Goldberg, and A. D. Shapere, Phys. Rev. D **65**, 124027 (2002).
[16] P. Meade and L. Randall, J. High Energy Phys. 05 (2008) 003.
[17] L. A. Anchordoqui, J. L. Feng, H. Goldberg, and A. D. Shapere, Phys. Rev. D **68**, 104025 (2003).
[18] L. A. Anchordoqui, J. L. Feng, H. Goldberg, and A. D. Shapere, Phys. Lett. B **594**, 363 (2004).
[19] D. M. Gingrich, Int. J. Mod. Phys. A **21**, 6653 (2006).
[20] M. J. Bowick, L. Smolin, and L. C. R. Wijewardhana, Phys. Rev. Lett. **56**, 424 (1986).
[21] S. Dimopoulos and R. Emparan, Phys. Lett. B **526**, 393 (2002).
[22] K. Cheung, Phys. Rev. D **66**, 036007 (2002).
[23] A. Chamblin and G. C. Nayak, Phys. Rev. D **66**, 091901 (R) (2002).
[24] S. Cullen, M. Perelstein, and M. E. Peskin, Phys. Rev. D **62**, 055012 (2000).
[25] P. Burikham, T. Figy, and T. Han, Phys. Rev. D **71**, 016005 (2005); **71**, 019905(E) (2005).
[26] L. A. Anchordoqui, H. Goldberg, S. Nawata, and T. R. Taylor, Phys. Rev. Lett. **100**, 171603 (2008).
[27] L. A. Anchordoqui, H. Goldberg, S. Nawata, and T. R. Taylor, Phys. Rev. D **78**, 016005 (2008).
[28] L. A. Anchordoqui, H. Goldberg, D. Lüst, S. Nawata, S. Stieberger, and T. R. Taylor, arXiv:0808.0497v2.
[29] L. Anchordoqui, T. Han, D. Hooper, and S. Sarkar, Astropart. Phys. **25**, 14 (2006).
[30] C. Kokorelis, Nucl. Phys. **B677**, 115 (2004).
[31] D. Cremades, L. E. Ibáñez, and F. Marchesano, Nucl. Phys. **B643**, 93 (2002).
[32] L. Susskin, arXiv:hep-th/9309145v2.
[33] G. T. Horowitz and J. Polchinski, Phys. Rev. D **55**, 6189 (1997).
[34] J. D. Bekenstein, Phys. Rev. D **7**, 2333 (1973).
[35] E. Halyo, B. Kol, A. Rajaraman, and L. Susskin, Phys. Lett. B **401**, 15 (1997).
[36] S. N. Solodukhin, Phys. Rev. D **57**, 2410 (1998).
[37] G. T. Horowitz and J. Polchinski, Phys. Rev. D **57**, 2557 (1998).
[38] T. Damour and G. Veneziano, Nucl. Phys. **B568**, 93 (2000).
[39] D. Amati, M. Ciafaloni, and G. Veneziano, Phys. Lett. B **197**, 81 (1987).
[40] J. Paton and C. Hong-Mo, Nucl. Phys. **B10**, 516 (1969).
[41] D. Amati and J. G. Russo, Phys. Lett. B **454**, 207 (1999).
[42] R. Emparan, G. T. Horowitz, and R. C. Myers, Phys. Rev. Lett. **85**, 499 (2000).
[43] V. Cardoso, M. Cavaglià, and L. Gualtieri, J. High Energy Phys. 02 (2006) 021.
[44] D. M. Gingrich, J. High Energy Phys. 11 (2007) 064.
[45] M. Fairbairn, J. Phys. A **39**, 1009 (2006).
[46] J. Pumplin, D. Stump, J. Huston, H. L. Lai, P. Nadolsky, and W. K. Tung, J. High Energy Phys. 07 (2002) 012.
[47] *LHAPDF the Les Houches Accord PDF Interface*, http://hepforge.cedar.ac.uk/lhapdf/.
[48] ATLAS Collaboration, Report No. CERN-OPEN-2008-020, 2008 (unpublished).
[49] C. M. Harris, P. Richardson, and B. R. Webber, J. High Energy Phys. 08 (2003) 033.
[50] J. Polchinski, Phys. Rev. Lett. **75**, 4724 (1995).
[51] S. de Alwis, Phys. Lett. B **388**, 291 (1996).